Efforts to Find Stick-Slip Flow in the Land of a Die under Sharkskin Melt Fracture Conditions: Polybutadiene

Yong Woo Inn[a)], Liangshi Wang[a)] and Montgomery T. Shaw[a,b)] *

Department of Chemical Engineering[b)] and Polymer Program[a)], Institute of Materials Science, University of Connecticut, Storrs, CT 06269-3136 USA

SUMMARY: Because stick-slip or other flow disturbances inside the die land have been suggested as a possible mechanism of the sharkskin, our effort was to observe any relevant periodic changes inside the die land during the sharkskin condition. We used particle tracking and time-resolved birefringence and two-dimensional light scattering in conjunction with a slit die attached to an extruder and a tubular glass die attached to a pressurized reservoir. Both dies could be observed up to the exit; both could also be directly observed downstream of the exit. While periodicities were easily seen in the slip-stick regime, none of the methods revealed any periodicity in the sharkskin regime. Direct observation of the sharkskin formation outside the die suggests a tearing and rolling mechanism as the origin of the sharkskin ridges found on polybutadiene extrudates.

Introduction

The sharkskin surface fracture phenomenon encountered in polymer extrusion is a critical problem in industry because the onset of sharkskin can be the limiting factor for higher production rates. It is also an challenging scientific problem because, despite much experimental and theoretical effort, the origin of sharkskin is still open to question. A central question concerns the spatial origin of sharkskin. Three possible sites have been suggested: an instability at the die entrance, stick-slip in the die land, and stretching at the die exit. The entrance instability hypothesis was suggested by Tordella[1)] den Otter[2)] and Weill[3)]. However, recent studies of the sharkskin characteristics have led to the rejection of this premise. Therefore many researches have been focused on the other two hypotheses of the spatial origin of sharkskin.

The hypothesis of stretching at the die exit has been mainly suggested after the visual observation of sharkskin development on polybutadiene (PBD) or polydimethyl siloxane (PDMS) extrusion (e.g., Howell and Benbow[4)], Cogswell[5)], El Kissi and Piau [6)], Inn et al. [7)]). By studying the extrusion behavior of linear low density polyethylene (LLDPE), Kurtz [8)] and Wang et al.[9)] also suggested that the sharkskin may be initiated at the die exit.

 CCC 1022-1360/00/$ 17.50+.50/0

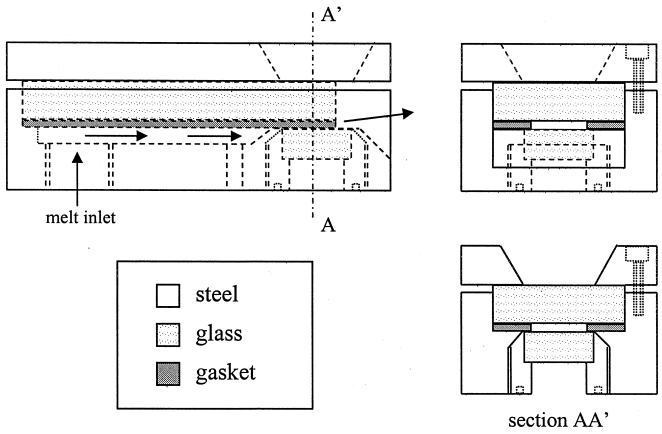

Fig. 1: Design of slit die for optical studies. The pressure transducer is located at the hole just upstream of the contraction leading to the land.

The hypothesis of stick-slip in the die land was motivated by reported observations that the sharkskin melt fracture coincides with a kink in the flow curve at about 0.1 MPa of shear stress for LLDPE. The slope change in the flow curve was explained by wall slip. The slip hypothesis was supported by observing the effect of different metallic die walls of various interfacial energy (Ramamurthy[10], Kalika and Denn[11], Person and Denn[12]). This seeming coincidence of three effects–sharkskin, flow-curve transition, and wall slip–brought a great deal of scientific attention. For this and other reasons, the slip at the wall of polymeric melt became one of the most important and controversial issues in rheology. Most of the wall-slip studies have used indirect methods based on rheological measurements. There are only few direct observations of the wall slip at high stresses associated with the spurt region, and any direct observations of the wall slip during sharkskin have not been reported.

In this study, our efforts were concentrated on observing any flow disturbance in the die land during sharkskin. We used small-angle-light scattering (SALS), flow birefringence and particle tracking. The material was polybutadiene (PBD). The advantages of using PBD are that it can be extruded at a low temperature, it develops big and slow sharkskin waves, and it has high enough stress-optical coefficient for the rheo-optical studies. The observed flow curve and fracture behavior of PBD agree with previous results reported by Bartôs and Homolek[13], Vinogradov et al.[14-16], Lim and Schowalter[17], and Piau et al.[18], and are very similar to those for LLDPE.

Experimental

Materials

We used polybutadiene (PBD) from Firestone Diene 35AC10, with reported M_w = 182,000 and M_w/M_n = 1.87. Air bubbles trapped inside PBD rubber were removed under vacuum at 50 °C. Rheological characterization has been described previously[7].

Extrusion Procedures

Two experimental setups were used. The first comprised a slit die attached a 3/4-in. Brabender single-screw extruder operated at 50 °C. The slit die featured glass walls that could be offset, as shown in Fig. 1. The dimensions of the land region of the slit die were length L = 30 mm, width W = 25 mm and gap H = 2 mm. Pressure was measured by a calibrated 3,000 psig melt pressure transducer (ISI 0613-3). The pressure signal was transferred to a PC with an A/D card for processing. The apparent wall shear stress σ_w was estimated from the average inlet pressure ΔP according to $\sigma_w = (H/2L)\Delta P$.

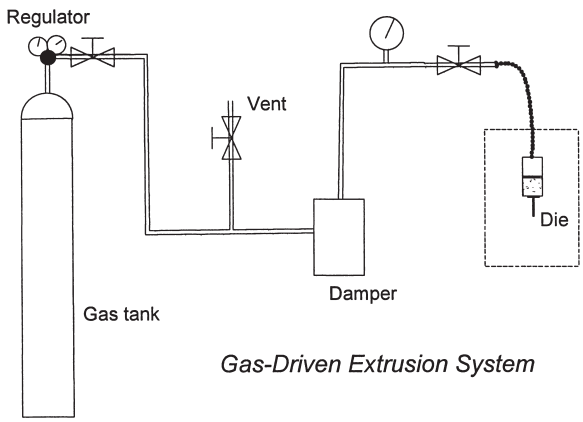

Fig. 2: Overall arrangement for gas-driven extrusion.

The second setup was designed to avoid the pressure fluctuations associated with screw extrusion. It comprised a gas delivery system and a polymer reservoir, with the gas and polymer separated by a diaphragm. The overall arrangement is shown in Fig. 2. The reservoir was connected to a die that could be easily changed. For optical observations the die featured

a glass insert that protruded from a steel holder, the latter providing the connection to the reservoir.

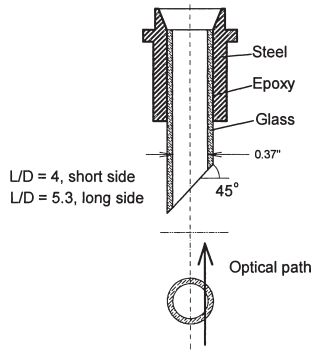

Fig. 3: Tubular glass die connected to gas-pressurized reservoir. Other dies were also used (e.g., see Fig. 5).

The geometry is shown in Fig. 3. Note that the die shown is cut at an angle of 45° to provide a maximum shear stress on the short side. This allows one side of the large strand to be free of sharkskin and prevents the pulling exerted by the material outside the die on that inside.

Design of rheo-optical setup

For both dies the optical setup was similar (Fig. 4). An optical bench was installed inside a darkbox to attach to the extruder or the gas-pressurized reservoir. The light source was a 10-mW He-Ne laser (Uniphase, 1105) with a wavelength of 632.8 nm. For the two-dimensional light scattering experiments, the scattering pattern was projected on a translucent screen and recorded by a camera. For the time-resolved light scattering and birefringence, the screen was replaced with a fiber optic connected to a photo-multiplier tube (Thorn EMI, RFI/S).

Particle tracking

Mica flakes coated with titanium dioxide (Mearl Corp, Mearlin Micro Gold 9260M) having size between 2 and 24 μm and thickness of approximately 0.3 μm were added to the PBD melt. Most of the mica flakes were removed from the die by flushing out with pure PBD. Then, a few, isolated, slow-moving particles near the die wall were monitored by a monochrome CCD camera (Elmo, SE360) fitted with macro lenses, and recorded by a S-VHS

VCR (Panasonic, AG1310). A fiber optic light source was used to illuminate the mica flakes. Due to vibration of the extruder, a small scratch was made on the glass wall to resolve the absolute motion of a slow-moving flake. Quality of the analog output from the videotape was adequate for digitization. A frame grabber (Snappy) captured frames of 640×480 pixels with an 8-bit gray scale.

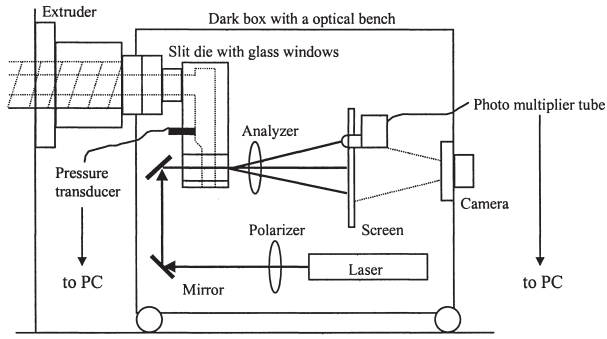

Fig. 4 Typical optical setup for time-resolved birefringence and scattering studies, as well as for two-dimensional light scattering.

Results and Discussion

General Observations

Observations of sharkskin phenomena using PBD have been published[7], and suggest a tearing action outside the die. With the very steady flow from the gas-driven extruder, the tearing and peeling action are particularly graphic. Figure 5 is a view of one of these peels as it rolls up onto the slow-moving surface of the strand before being dragged downstream as the velocity profile flattens.

Rheo-optical studies

If there are periodic disturbances in the flow near the die land surface, which could be the origin of the sharkskin melt fracture, it is expected that there would be corresponding disturbances in the intensity of scattered light and transmitted light through crossed polarizers. With static, two-dimensional light scattering, one would expect that the scattering pattern would be asymmetrical, corresponding to the symmetry of the flow disturbance. However,

little is known in advance about the symmetry or size of the orientation fluctuations that would lead to such a pattern. If the size scale were the same as the melt fracture, then the scattering pattern would exhibit asymmetry only at extremely small angles, which were beyond the capabilities of the available equipment.

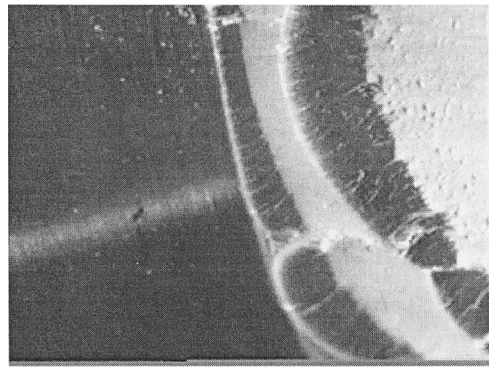

Fig. 5. View of sharkskin ridge forming on extrudate emerging from round die attached to gas-driven reservoir. Flow is from left to right. The edge of the die on the left is very sharp, which prevents the roll from hitting the die as it rolls backward.

The time-resolved techniques were more successful in that signals were obtained with expected behavior. A startup of a time-resolved birefringence experiment is shown in Fig. 6.

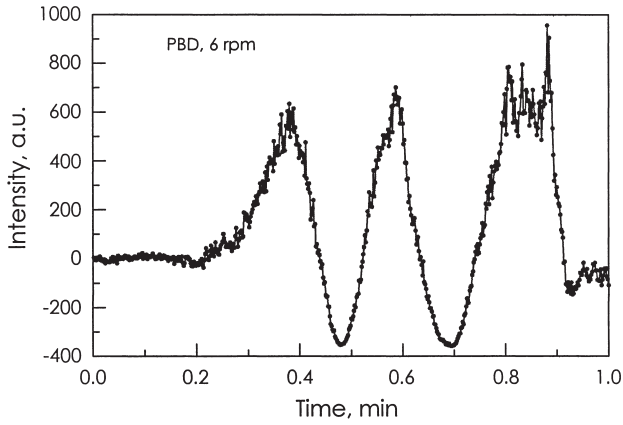

Fig. 6: Startup of a time-resolved birefringence experiment showing the progression through the orders of retardance. Slit die, 50 °C, 6 rpm screw speed, PBD.

The anticipation was that the information concerning sharkskin would appear in areas such as the top part of the third peak of Fig. 6, where there is apparently a higher frequency of around 1 Hz. Thus the strategy was to stabilize the pressure at various degrees of retardance, and gather intensity vs. time files. These were then transformed to the frequency domain with the thought that the resulting spectrum could be compared with the known sharkskin frequency (Fig. 7).

An typical plot of intensity vs. time for a typical run using the slit die is shown in Fig. 8. Included in this graph is the corresponding stress, as estimated from the pressure transducer reading and the equation given previously. Under these conditions prominent sharkskin is observed as the melt exits the die.

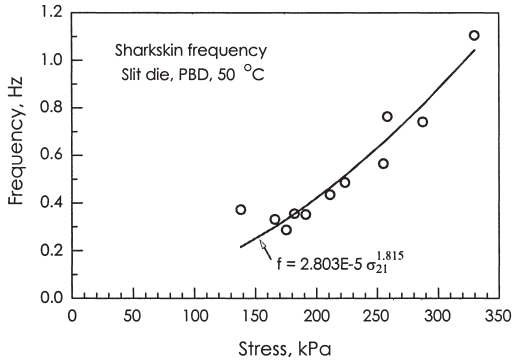

Fig 7: Sharkskin frequency dependence on shear stress. The curve is a nearly quadratic, which has been reported by others [19].

A transform to the frequency domain is shown in Fig. 9; as can be seen, there is little but noise in the spectrum.

A typical result from the particle tracking experiments is depicted in Fig. 10, which shows the velocity of the particle over a span of 24 s as it approached the die exit. The velocity measured puts the particle at about 70 μm away from the wall for the conditions of the extrusion. While at first glance there appears to be some periodicity in the velocity, such was not confirmed by analysis in either the time or frequency domain. The former was effected by subtracting a quadratic from the data and examining the residuals for too few or too many runs, i.e., sequences of positive or negative residuals. The results are shown in Table 1 for too many runs; while the number of runs is large, the probably of still more is judged high enough

to reach the "not significant" conclusion. The FT of the velocity to the frequency domain revealed no harmonics near the sharkskin frequency.

Table 1. Particle velocity fluctuations, residual runs analysis (test for too many runs).

Points	Runs	Z statistic	Probability	Conclusion
49	30	1.62	0.052[a)]	Not significant

[a)] Probability of a larger number of runs than that observed is 5.2%

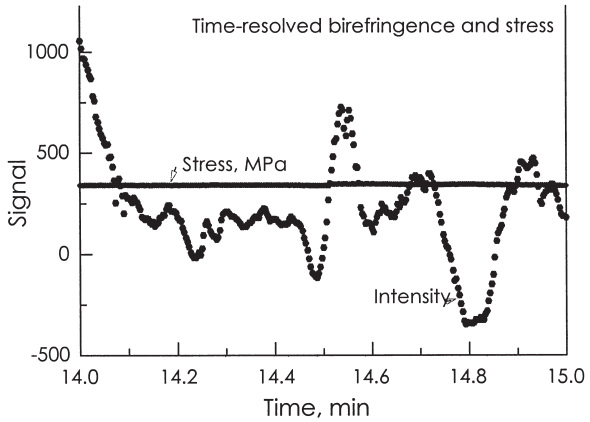

Fig. 8: Stress and optical intensity for a 1-min segment taken from a run in the slit die at 50 C with PBD. The optical path, 1 mm above the die exit, was set up for birefringence with polarizers at -45° and +45° and with the detector on axis.

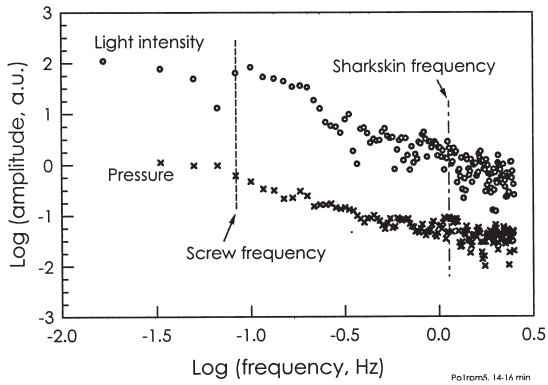

Fig. 9: FT of the data in Fig. 8.

With the tube die, results were similar. Figure 11 shows the transform of the data taken at 86 kPa, which gives distinct sharkskin features at a low frequency of about 0.1 Hz (Fig. 12). While Fig. 11 suggests a broad band of intensity fluctuations centered on this frequency, windowing of the data removes this band completely.

The lack of evidence of disturbance inside the die, in spite of strong sharkskin just downstream, is to some extent different from the result of Barone and Wang[19], who reported an oscillation in the birefringence in a slit die during sharkskin melt fracture. A possible explanation is the slight, but important, difference in geometry. The offset faces of the die used in this work reduce the pulling of the fractured extrudate on the melt inside, thus reducing this source of birefringence change.

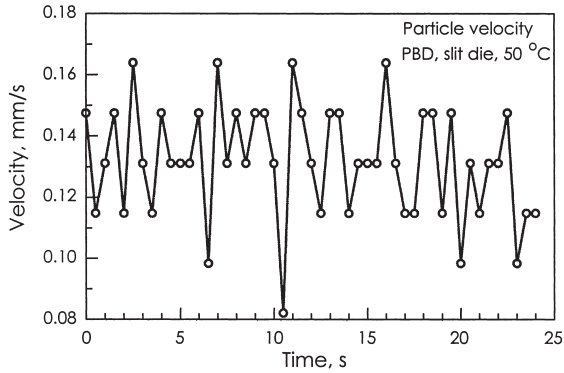

Fig. 10: Velocity of particle (~10-μm mica flake) as it approaches the die exit. Particle is about 70 μm away from the wall. Stress is about 210 kPa.

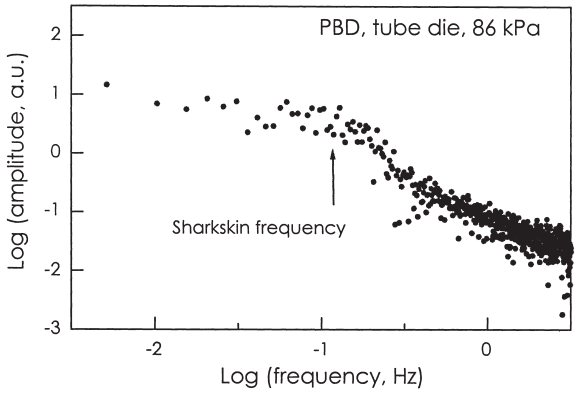

Fig. 11: Transform of intensity data for tube flow of PBD using polarized light. Light enters near shortest side of tube (see Fig. 3). Polarizers are at 0 and 90°.

Conclusions

The sharkskin melt fracture of polybutadiene (PBD) melt was studied in a variety of geometries over the entire stress range corresponding to melt fracture. Time-resolved birefringence and light scattering, as well as direct particle tracing were used in an attempt to find periodic slip that would correspond to the very visible sharkskin melt fracture seen at the exit. The results of all methods that were attempted in this study were negative, implying that the entire sharkskin process is external to the die or that the disturbance leading up to fracture is aperiodic. The latter possibility is being pursued by recording the local melt fracture peaks and valleys, and correlating these with the signals detected inside the die.

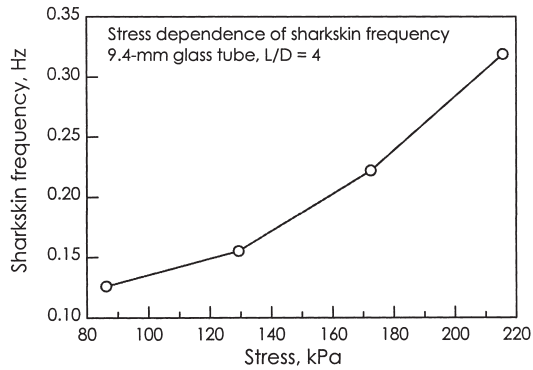

Fig. 12: Stress dependence of the sharkskin frequency in glass tube die (Fig. 3).

Acknowledgements

This work was supported by the National Science Foundation, DMI-9422108. Valuable technical assistance with the experiments was provided by Denise E. Packard, Matthew Daly and Jamie Hubbard.

References

1. J. P. Tordella, Rheol. Acta 1, 216 (1958)
2. J. L. den Otter, Plastics & Polymers, June 155 (1970)
3. A. Weill, Rheol. Acta 19, 623 (1980)
4. E. R. Howell, J. J. Benbow, Trans. J. Plastics Inst. 30, 240 (1962)
5. F. N. Cogswell, *J. Non-Newtonian Fluid Mech.* **2**, 37 (1977)
6. N. El Kissi, J.M. Piau, *J. Non-Newtonian Fluid Mech.* **37**, 55 (1990)
7. Y. W. Inn, R. J. Fisher, M. T. Shaw. *Rheol. Acta* **37**, 573 (1998)
8. S. J. Kurtz in: Advances in Rheology, Vol. 3, B. Mena, A. Gracia-Rejon and C. Rangel-Nafaile, (Eds.) Universidad Nacional Autonoma de Mexico, 1984, pp.399ff
9. S. Q. Wang, P. A. Drda, Y.-W. Inn, J. Rheol. 40, 875 (1996)
10. A. V. Ramamurthy, *J Rheol.* **30**, 337 (1986)
11. D. S. Kalika, M. M. Denn, *J Rheol.* **31**, 815 (1987)
12. T. J. Person., M. M. Denn, *J Rheol.* **41**, 249 (1997)
13. O. Bartôs, J. Holomek, *Polym. Eng. Sci.* **11**, 324(1971)
14. G. V. Vinogradov, *Rheol. Acta* **12**, 357 (1973)
15. G. V. Vinogradov, *Polymer* **18**, 1275 (1977)
16. G. V. Vinogradov, V. P. Protasov, V. E. Dreval, *Rheol. Acta* **23**, 46 (1984)
17. F. J. Lim, W. R. Schowalter, *J. Rheol.* **33**, 1359 (1989)
18. J. M. Piau N. El Kissi, F. Toussaint, A. Mezghani, *Rheol. Acta* **34**, 40 (1995)
19. J. R. Barone, S.-Q. Wang, Paper IR6, Society of Rheology 70th Annual Meeting, October 4-8, 1998.